Iranian Journal of Basic Medical Sciences
ijbms.mums.ac.ir

Preparation, characterization, and comparison of the release of antibacterial peptide CM11 from PLGA nanoparticles and microparticles

Mohammadmahdi Eshaghi [1], Mehrdad Moosazadeh Moghaddam [2], Marzieh Dehghani [3], Nematollah Jonaidi-Jafari [4], Hamid Hesarikia [5], Ramezan Ali Taheri [1]*

[1] Nanobiotechnology Research Center, New Health Technologies Institute, Baqiyatallah University of Medical Sciences, Tehran, Iran
[2] Tissue Engineering and Regenerative Medicine Research Center, New Health Technologies Institute, Baqiyatallah University of Medical Sciences, Tehran, Iran
[3] Department of Biophysics, College of Biological Sciences, Tarbiat Modares University, Tehran, Iran
[4] Health Management Research Center, Lifestyle and Spiritual Health Research Institute, Baqiyatallah University of Medical Sciences, Tehran, Iran
[5] Trauma Research Center, Clinical Sciences Institute, Baqiyatallah University of Medical Sciences, Tehran, Iran

ARTICLE INFO

Article type:
Original

Article history:
Received: May 3, 2026
Accepted: Jun 21, 2026

Keywords:
Antimicrobial peptide
Biofilms
Nanomedicine
Polylactic acid-polyglycolic-acid copolymer
Pseudomonas aeruginosa

ABSTRACT

Objective(s): *Pseudomonas aeruginosa* (*P. aeruginosa*) is a Gram-negative bacterium capable of causing acute and chronic infections. Treating these infections is increasingly challenging as this bacterium develops antibiotic resistance. Antimicrobial peptides (AMPs) have emerged as promising therapeutic candidates due to their broad-spectrum activity. Cecropin-Melittin-11 (CM11), a cationic AMP, has shown antimicrobial activity against various pathogens. However, the progression of AMPs from preclinical research to clinical applications is hindered by enzymatic degradation, short systemic half-life, and cytotoxicity. To overcome these challenges, poly(lactic-co-glycolic acid)(PLGA) particles for peptide delivery have gained attention.

Materials and Methods: CM11-loaded PLGA nanoparticles (NPCM11) and microparticles (MPCM11) were prepared using a double-emulsion solvent evaporation (W1/O/W2) method and characterized for particle size, morphology, encapsulation efficiency, and *in vitro* release. Their antibacterial activity against planktonic and biofilm-forming *P. aeruginosa* was evaluated using broth microdilution assay. Their cytocompatibility was evaluated using 3-(4,5-Dimethylthiazol-2-yl)-2,5-Diphenyltetrazolium Bromide (MTT) assay.

Results: Optimum formulations of NPCM11 and MPCM11 were synthesized, exhibiting spherical morphology with average sizes of 281 nm and 7.63 µm, respectively. The encapsulation efficiency (EE%) of NPCM11 and MPCM11 was 63.5% and 60.3%, respectively, while the *in vitro* CM11 release was 82% and 58%. According to broth microdilution and biofilm inhibition assays, NPCM11 outperformed free CM11 and MPCM11 against planktonic bacteria, whereas both NPCM11 and MPCM11 were superior to free CM11 in biofilm inhibition. MTT assay revealed that NPCM11 and MPCM11 significantly reduced CM11 cytotoxicity.

Conclusion: Overall, NPCM11 and MPCM11 were promising formulations of CM11 for treating *P. aeruginosa* infections.

Corrected Proof

▶ Please cite this article as:
Eshaghi M, Moosazadeh Moghaddam M, Dehghani M, Jonaidi-Jafarid N, Hesarikia H, Taheri RA. Preparation, characterization, and comparison of the release of antibacterial peptide CM11 from PLGA nanoparticles and microparticles. Iran J Basic Med Sci 2026; 29:

Introduction

The emergence of antibiotic resistance is a serious threat to global health. The mortality rate from antibiotic-resistant bacterial infections is expected to reach 39 million people within the next 25 years. These forecasts underscore the need to develop novel and effective antimicrobial therapeutics (1). *Pseudomonas aeruginosa* is a Gram-negative, rod-shaped bacterium commonly found in freshwater reservoirs and capable of causing acute and chronic infections, especially in immunocompromised hosts with a variety of diseases, such as cancer, AIDS, cystic fibrosis, burns, neutropenia, and bronchiectasis. *P. aeruginosa* also poses a serious threat to patients who undergo surgery and receive implant-based treatments, as this strain is highly inclined to form biofilms (2, 3). Treating related infections is becoming increasingly challenging as this bacterium develops antibiotic resistance through several mechanisms, including intrinsic antibiotic resistance (restricted membrane permeability), antibiotic-inactivating enzymes, and efflux systems. The issue of antibiotic resistance is further aggravated in cases of biofilm formation, e.g., in cystic fibrosis and other lung-related diseases. Biofilms are associated with approximately 65% of bacterial infections. The World Health Organization (WHO) has identified *P. aeruginosa* among the top three important antibiotic-resistant microbial strains (3, 4).

Antimicrobial peptides (AMPs) have emerged as

***Corresponding author:** Ramezan Ali Taheri. Nanobiotechnology Research Center, New Health Technologies Institute, Baqiyatallah University of Medical Sciences, Tehran, Iran. Email: taheri@bmsu.ac.ir

© 2026. This work is openly licensed via CC BY 4.0.
This is an Open Access article distributed under the terms of the Creative Commons Attribution License (https://creativecommons.org/licenses), which permits unrestricted use, distribution, and reproduction in any medium, provided the original work is properly cited.

promising therapeutic candidates for microbial infections due to their broad-spectrum activity and various mechanisms of action, which reduce the likelihood of resistance development (5, 6). Contrary to conventional antimicrobial drugs, AMPs employ multiple mechanisms, including disruption of intracellular metabolic pathways, membrane lysis, and biofilm formation inhibition, to hinder bacterial infection. This diversity in mechanisms of action makes it difficult for bacterial strains to develop resistance to AMPs. Moreover, use of AMPs in combination with conventional antimicrobial drugs has been shown to resensitize resistant strains to those drugs (7, 8).

Among AMPs, CM11—a cationic hybrid peptide derived from cecropin A and melittin—has shown potent antimicrobial activity against a wide range of pathogens. CM11 comprises 11 amino acids. It was designed to be less cytotoxic than both cecropin A and melittin while retaining their antimicrobial effectiveness. Its short amino acid sequence also makes production cost-effective. However, the progression of AMPs like CM11 from preclinical research to clinical application is hindered by susceptibility to enzymatic degradation, a short systemic half-life, and potential cytotoxicity at high concentrations (9-12).

To overcome these challenges, biodegradable polymeric carriers for controlled peptide delivery have gained significant attention. PLGA, an FDA-approved polymer, offers biocompatibility, tunable degradation rates, and proven efficacy as a drug delivery vehicle (13). Encapsulation of AMPs in PLGA nanoparticles (NPs) and microparticles (MPs) can protect them from premature degradation and enhance bioavailability (14-17). However, studies directly comparing PLGA NPs and MPs for AMP delivery are relatively limited, and such comparisons have not been reported for CM11 to the best of our knowledge.

This study addresses this gap by comparatively evaluating NPCM11 and MPCM11 for treating acute and chronic bacterial infections caused by *P. aeruginosa*. We hypothesize that the difference in rate of CM11 release from NPCM11 and MPCM11 determines their suitability for treating acute or chronic infections, characterized by planktonic bacteria and biofilms, respectively. The literature reports that PLGA NPs release their payload faster than MPs due to a smaller hydrodynamic size (18-20). We hypothesize that this increased rate of release renders NPs more suitable for acute infections, where a high concentration of drug is needed at the site of infection to immediately hinder the spread of planktonic microbial cells (20, 21). On the other hand, MPs, which depict a more sustained release profile, are hypothesized to be more suitable for treating chronic conditions characterized by biofilm formation (21-23) by maintaining a high drug concentration for a longer duration.

PLGA NPs and MPs were synthesized using a W1/O/W2 method, and their physicochemical properties were characterized by dynamic light scattering (DLS), Fourier transform infrared (FTIR) spectroscopy, and field emission scanning electron microscopy (FESEM). The in vitro release of CM11 from NPCM11 and MPCM11 was evaluated to elucidate the influence of particle size on peptide release. Furthermore, antibacterial activity was assessed using a broth microdilution assay and a biofilm inhibition assay. Finally, the cytocompatibility of NPCM11 and MPCM11 was examined via an MTT assay. By comparing the performance of NPCM11 and MPCM11, this study provides insights into the potential applications of PLGA NPs and MPs for the treatment of acute and chronic P. aeruginosa infections.

Materials and Methods

Materials

PLGA (50:50, MW=30-60 kDa), ethyl acetate, phosphate-buffered saline (PBS), MTT, and polyvinyl alcohol (PVA, MW=72 kDa) were purchased from Merck Co., Germany. CM11 was kindly provided by our colleague, Dr. Mehrdad Moosazadeh Moghaddam (GenScript Co., China). The Human Foreskin Fibroblasts (HFF) cell line was kindly provided by our colleague, Dr. Marzieh Dehghani (Obtained from Motamed Cancer Research Institute, Iran).

Particle synthesis

A series of experiments was designed using the single-factor analysis approach to optimize the W1/O/W2 method for synthesizing NPCM11 and MPCM11 within suitable size ranges. The studied parameters included oil-to-secondary aqueous phase volume ratio (O:W2), PLGA concentration (mg/mL), PVA concentration (%w/v), ultrasonic probe power input (W), and duration (t_s). Fixed values were assigned to other parameters, including centrifugation speed and time, sonication cycle, and primary aqueous-to-oil volume phase ratio (W1:O). The range of values for the parameters analyzed by the single-factor method and the values of fixed parameters were determined through extensive literature review (18-20, 24-28).

To prepare NPCM11 and MPCM11, PLGA was initially dissolved in ethyl acetate by vigorous vortex mixing. The primary aqueous phase was gradually added to the oil phase, and the W1/O emulsion was formed by an additional 10 s of vortex mixing (W1:O=0.1, CM11 Concentration: 500 µg/ml). The emulsion was then subjected to probe-mediated ultrasonication (sonication cycle=0.7) in 10-second intervals with cooling breaks in an ice bath. Next, the emulsion was gradually added to a secondary aqueous phase containing PVA under stirring. For the next step, in the case of NPCM11, the resulting W1/O/W2 emulsion was immediately subjected to probe-mediated ultrasonication (sonication cycle=0.7) in 10-second intervals with cooling breaks in an ice bath. For MPCM11, this step was skipped, and the double emulsion was vortexed for only 10 sec. The emulsion was then stirred overnight to allow complete evaporation of ethyl acetate and hardening of the PLGA particles. To remove impurities, the emulsion was centrifuged (For NPs: 18000 g, 20 minutes – For MPs: 5000 g, 20 minutes) at 4 ˚C. The supernatant was removed for calculating EE% and loading capacity (LC%). The precipitate was resuspended in distilled water or PBS by vigorous vortexing.

Particle characterization

NPCM11 and MPCM11 sizes were determined using DLS by a Malvern Zetasizer Nano ZS instrument and FESEM by a TESCAN Mira2 instrument, respectively. The criterion for an optimized monodisperse NPCM11 formulation was a polydispersity index (PDI) below 0.1, which is an acceptable upper limit for Z-average reliability. Because DLS is not suitable for accurately measuring micron-sized particles, it was used only as a screening tool to identify MPCM11 formulations for subsequent FESEM analysis (29).

NPCM11 and MPCM11 morphology was studied using

Corrected Proof

FESEM. The samples for FESEM were prepared by the air-drying method. A droplet of each sample was placed on a microscope slide and allowed to air-dry under a fume hood. The samples were then coated with a layer of gold for enhanced electron conductivity and image resolution.

To calculate synthesis yield, MPCM11 and NPCM11 solutions were freeze-dried after centrifugation, and their weight was compared with the initial PLGA+CM11 weight. To evaluate particle stability during storage in aqueous suspension, the Z-average and PDI of the optimized NPCM11 sample were monitored for a month. For MPCM11 stability assessment, FESEM images were taken after a month.

CM11 encapsulation

To calculate EE% and LC% of CM11, the supernatant from centrifuged samples was extracted, which contained unloaded CM11. By subtracting the amount of unloaded CM11 from its initial amount, EE% and LC% were calculated using equations 1 and 2, respectively. In these equations, LD denotes the weight of loaded CM11, which was calculated by subtracting the weight of unloaded CM11 from its initial weight (ID). P denotes the weight of PLGA used in the synthesis protocol.

$$EE\%=(LD/ID)\times100\% \quad (1)$$
$$LC\%=(LD/(P+LD))\times100\% \quad (2)$$

To determine the amount of unloaded CM11 from the supernatant, the absorbance of the samples was read at 278 nm using UV-visible spectroscopy. CM11 demonstrates a sharp peak at this wavelength. To correlate absorbance and CM11 concentration, a calibration curve was produced using absorbance-concentration data from a series of CM11 samples with known concentrations.

To qualitatively verify CM11 encapsulation within PLGA particles, FTIR spectroscopy was used. Dry samples of PLGA, blank NP (NP-blank), blank MP (MP-blank), NPCM11, and MPCM11 were analyzed.

In vitro CM11 release

Equal concentrations of NPCM11 and MPCM11 were suspended in multiple microtubes containing 1 cc PBS (pH 7.4) and incubated in an incubation shaker at 37 ˚C (180 rpm). At each predetermined time point, a microtube was removed and centrifuged (18000 g, 20 min). Supernatant, which contained the released CM11, was extracted and its absorbance was read at 278 nm to determine the concentration of released CM11 at the given time point.

Broth microdilution and biofilm inhibition assay

To determine the values of minimum inhibitory concentration (MIC) and minimum bactericidal concentration (MBC) for free CM11, NP-blank, MP-blank, NPCM11, and MPCM11, a broth microdilution assay was performed for *Escherichia coli* (ATCC 25922), *Staphylococcus aureus* (ATCC 25923), and *P. aeruginosa* (ATCC 27853) according to CLSI protocols in U-bottom 96-well plates (30). Isolated colonies of each strain from 24-hr incubated agar plates were suspended in a saline solution, and turbidity was adjusted to 0.5 McFarland standard (equal to 1×10^8 CFU/ml). This suspension was diluted 1:20 to yield 5×10^6 CFU/ml, and 0.01 of the resulting suspension was used to inoculate the wells (final bacterial concentration: 5×10^4 CFU/well). The standardized suspensions were used to inoculate 96-well plates (10 µl/well). Stock solutions of each formulation in Mueller-Hinton broth (MHB) were prepared by dissolving freeze-dried samples at the highest tested concentration and diluted two-fold in the adjacent wells until reaching 1 µg/ml in the final well. The final concentration of standardized suspensions of free CM11, NPCM11, and MPCM11 was 256 µg/ml in terms of CM11 concentration. The final concentration of standardized suspensions of NP-blank and MP-blank was 14 mg/ml in terms of PLGA concentration. Each well contained a total volume of 200 µl. The positive control group consisted of wells inoculated with the standardized suspensions, without receiving any treatment from the prepared formulations. The positive control consisted of wells inoculated with the standardized suspensions of each strain, without receiving any treatment from the prepared formulations. The negative control consisted of wells with sterile medium. The purpose of the negative control was to ensure absence of any contamination. To elucidate the MIC, after 24 hr of incubation, the wells were stained with resazurin dye and incubated for an additional 2 hr. Samples from the MIC well and higher concentrations were used for MBC determination. To this end, 5 µl of each sample was poured on Mueller-Hinton agar (MHA)-containing plates of each strain and incubated for 24 hr.

To assess the capacity of the abovementioned formulations to inhibit *P. aeruginosa* biofilm formation, a crystal violet staining method was adopted from the literature (31). Briefly, an overnight culture of *P. aeruginosa* was diluted in fresh medium to the desired inoculum density (consistent with the 0.5 McFarland standard). The final concentration of standardized suspensions of free CM11, NPCM11, and MPCM11 was 128 µg/ml in terms of CM11 concentration. Similar to the broth microdilution assay, these suspensions were used to treat wells inoculated with *P. aeruginosa,* and serial dilutions of free CM11, NPCM11, and MPCM11 were prepared in sterile 96-well plates. After 24 hr of incubation under static conditions at 37 ˚C in flat-bottom 96-well plates, the well supernatants were removed to separate planktonic cells. The wells were then gently washed with distilled water three times and air-dried before being stained with 1% (w/v) crystal violet solution and incubated at room temperature for 15 min. Next, the wells were washed with distilled water to remove excess crystal violet. The stained biofilm was dissolved in 95% ethanol and transferred to new wells. The absorbance of the wells was read at 595 nm using an ELISA microplate reader. The percentage of biofilm growth in each well was calculated as the ratio of that well's absorbance to that of the positive control. The positive control consisted of wells inoculated with the standardized suspensions of *P. aeruginosa*, without receiving any treatment from the prepared formulations. The negative control consisted of wells with sterile medium. The purpose of the negative control group was to ensure the absence of any contamination.

MTT assay

To determine the cytotoxicity of free CM11, NP-blank, MP-blank, NPCM11, and MPCM11, an MTT assay was performed on the HFF cell line in a flat-bottom 96-well plate. In each well, 5000 cells were seeded using 200 µl of Dulbecco's

Corrected Proof

Table 1. Single-factor analysis for optimizing poly (lactic-co-glycolic acid) nanoparticles and microparticles

Test No.	O:W2 (V/V)	PLGA Conc. (mg/ml)	PVA (%W/V)	Ultrasonic power (watt)	Ultrasonic time (seconds)	Z-average (nm)	Polydispersity index (PDI)	Zeta potential (mV)
S1	0.5	10	1	200	120	281±13	0.05±0.03	-0.33±0.28
S2	0.5	10	2	200	120	368±18	0.24±0.07	-1.82±0.18
S3	0.2	10	1	200	120	460±23	0.24±0.11	-6.90±-2.03
S4	0.5	10	1	200	60	334±15	0.19±0.06	-0.85±0.33
S5	0.5	20	1	200	120	327±14	0.19±0.09	-3.15±0.62
S6	0.5	10	1	100	120	349±14	0.15±0.06	-1.98±0.49
S7	0.125	10	0.1	80	30	1539±152	0.94±0.05	-8.45±1.03
S8	0.2	20	0.1	80	30	323±13	0.17±0.04	-3.64±0.86
S9	0.2	20	0.1	Vortex only	Vortex only	1563±155	0.96±0.03	-2.35±0.52
S10	0.5	20	0.1	Vortex only	Vortex only	6384 ±442	0.48±0.19	-4.00±1.17
S11	0.5	20	1	Vortex only	Vortex only	5893±368	0.39±0.14	-1.81±0.41
S12	0.33	10	1	Vortex only	Vortex only	4650±315	0.46±0.18	-0.54±0.23

Modified Eagle Medium (DMEM) containing 10% fetal bovine serum (FBS) and 1% penicillin-streptomycin. The plate was incubated at 37 ˚C for 24 hr. After confirming cell attachment via optical microscopy, the medium was replaced with fresh medium containing the above-mentioned formulations. The fresh media were prepared by dissolving freeze-dried powders of each formulation in DMEM at the highest tested concentration. The lower concentrations were obtained using 2-fold dilutions. Following medium replacement, the plate was incubated for another 24 hr. Then, the medium was replaced with a mixture of MTT solution and fresh medium and incubated for an additional 4 hr. To dissolve the formed formazan crystals, dimethyl sulfoxide (DMSO) was added to the wells, and absorbance was read using an ELISA microplate reader at 570 nm. The positive control group contained cells without receiving any treatment. The negative control group contained blank medium without cells to ensure absence of contamination in the plate. Statistical analysis was performed using GraphPad Prism. Two-way ANOVA was used to conduct the analysis. Experiments were performed in triplicate. The alpha value was set at 0.05.

Results

Particle synthesis and characterization

NPCM11 and MPCM11 were prepared by the W1/O/W2 method, and the protocol's parameters were optimized using single-factor analysis. Table 1 shows the results of the analysis.

Tests No. 1 to 6 were performed to synthesize NPCM11 with minimum PDI and Z-average. According to the results, the sample from Test No. 1 (S1) was the optimum formulation with PDI=0.05, Z-average=281 nm, and zeta potential=-0.33 mV. Figure 1 presents FESEM images of S1, confirming the formation of spherical, monodisperse NPs.

Tests No. 7 to 12 were performed to synthesize MPCM11 with minimum PDI as the superior candidates for FESEM analysis. The sample from Test No. 11 (S11) with PDI=0.39

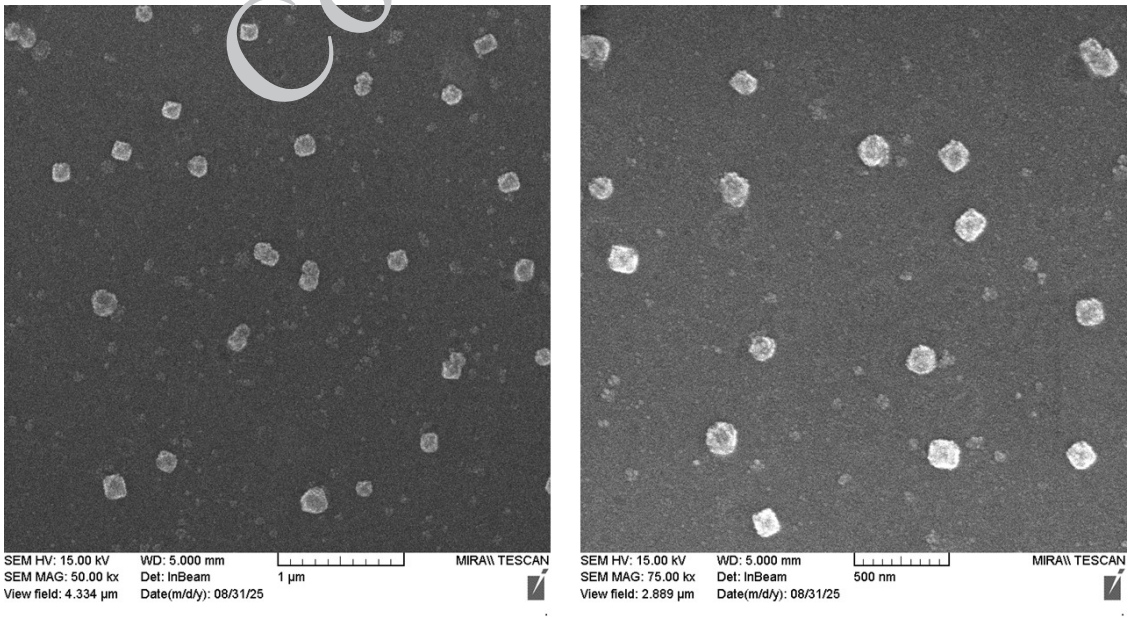

Figure 1. Field emission scanning electron microscopy images of S1 (optimized nanoparticle)–Left panel (scale bar=1 µm); Right panel (scale bar=500 nm)

Corrected Proof

was chosen for this purpose. Figure 2 presents FESEM images of S11, confirming the formation of spherical MPs with sizes ranging from 3 to 14 µm. The average size of S11 particles, calculated by measuring several particles from sample FESEM images, was 7.62 µm.

The yields of NPCM11 and MPCM11 were 73% and 93%, respectively. Because larger particles precipitate more readily during centrifugation, the higher yield of MPCM11 compared with NPCM11 was expected. To assess NPCM11 stability over time, S1 was analyzed by DLS after one week, two weeks, and four weeks, and the results are shown in Table 2. Figure 3 shows FESEM images of S1 after 1 month of storage in a refrigerator.

Table 2 shows that particle size and monodispersity were maintained over four weeks of storage, with no evidence of aggregation. The zeta potential remained near neutral throughout the four-week storage period. Figure 3 corroborates the DLS findings, showing that the particles retained their spherical morphology and nanoscale size after storage.

Table 2. Results of dynamic light scattering analysis for sample 1 over time

Week	Z-average	Polydispersity index (PDI)	Zeta potential (mV)
0	281±13	0.05±0.03	-0.33 ±0.28
1	274±18	0.05±0.02	-0.55±0.13
2	233±28	0.12±0.05	-2.31±0.43
4	269±16	0.05±0.02	-1.33±0.24

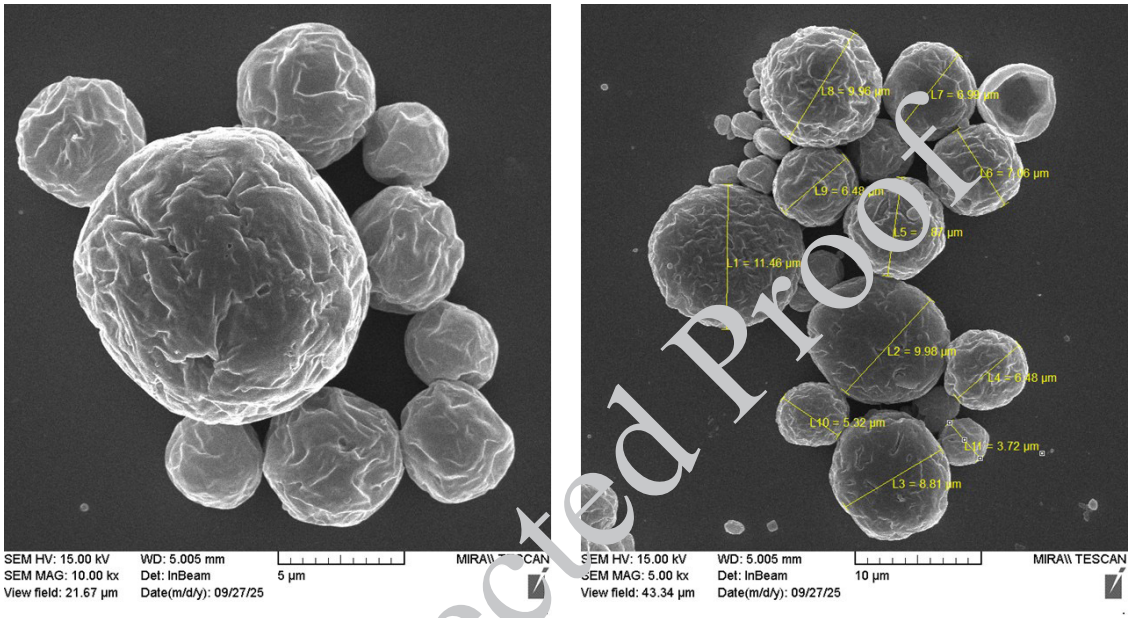

Figure 2. Field emission scanning electron microscopy image of sample 11 (optimized microparticle)–Left panel (scale bar=5 µm); Right panel (scale bar=10 µm)

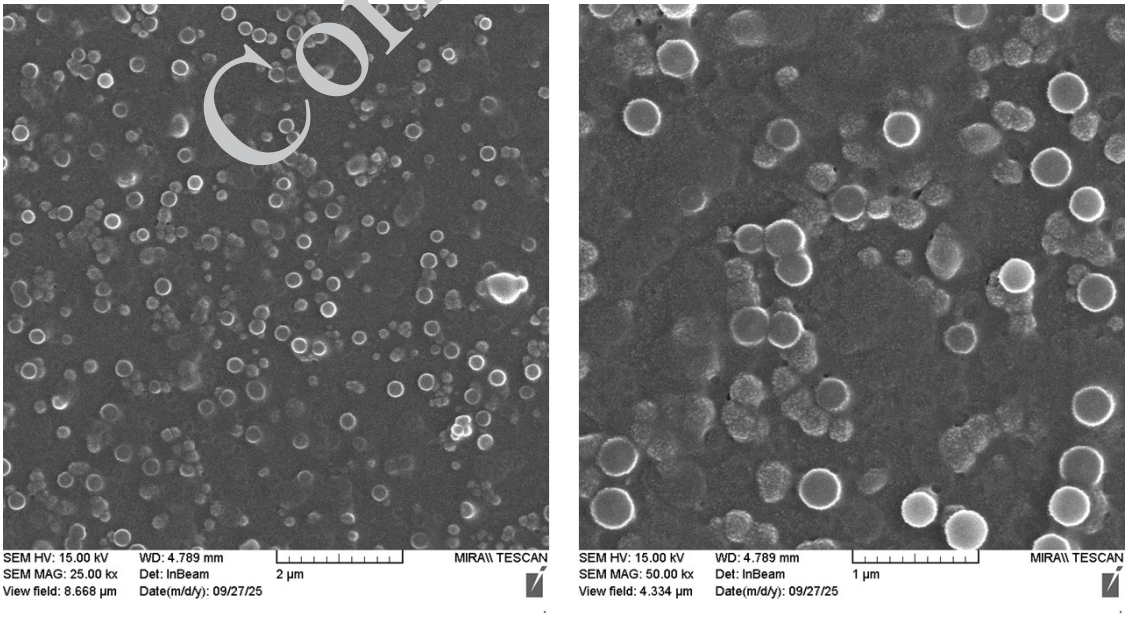

Figure 3. Field emission scanning electron microscopy images of sample 1 after four weeks in storage–Left panel (scale bar=2 µm); Right panel (scale bar=1 µm)

Corrected Proof

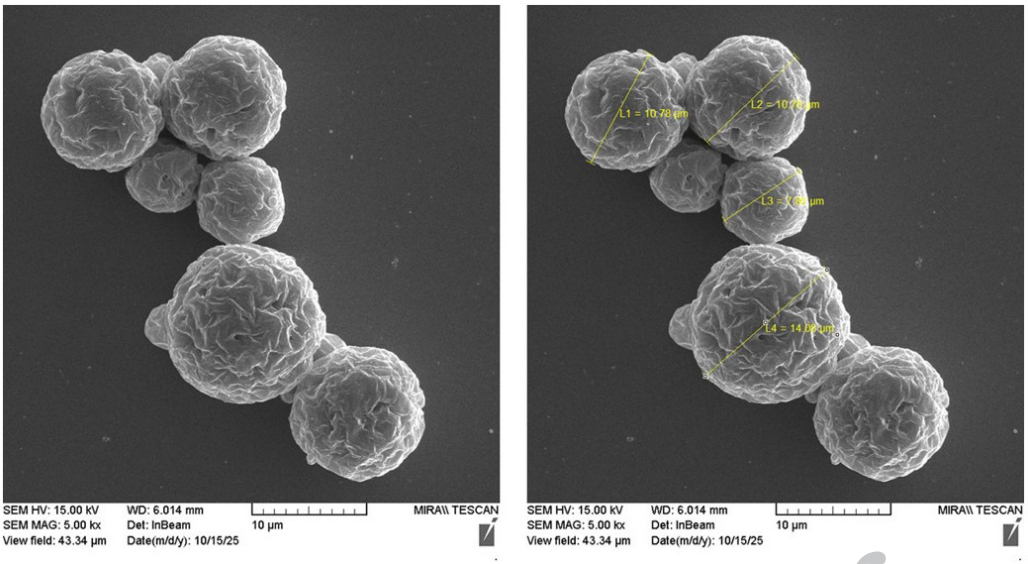

Figure 4. Field emission scanning electron microscopy images of sample 11 after four weeks in storage–Left panel (scale bar=10 µm); Right panel (scale bar=10 µm)

FESEM images of S11 were obtained after four weeks to evaluate MPCM11 stability (Figure 4). As shown in Figure 4, no noticeable changes in particle morphology, aggregation, or mean particle size were observed after one month of storage, indicating the physical stability of MPCM11.

CM11 encapsulation in PLGA NP and MP

To verify CM11 encapsulation, FTIR analysis was performed. Figure 5 demonstrates FTIR spectra of PLGA, NP-blank, MP-blank, NPCM11, and MPCM11. The characteristic FTIR bands for PLGA include C=O stretching at 1724 cm^{-1}, C-H stretching at 2865 and 2942 cm^{-1}, C=O bending at 1363, 1411, and 1467 cm^{-1}, and C-O stretching at 1101 and 1169 cm^{-1} (32, 33). These bands have been maintained in the spectra of NP-blank and MP-blank. In the spectra of NPCM11 and MPCM11, new bands appearing at 3300 cm^{-1} and 627 cm^{-1} indicate stretching and bending of the N-H bond, respectively (34, 35). These additional bands confirm the successful encapsulation of CM11.

To optimize EE% and LC%, different CM11:PLGA weight ratios (0.005, 0.01, 0.05) were used to synthesize NPCM11 and MPCM11. As shown in Table 3, EE% increases noticeably from CM11:PLGA=0.005 to 0.01 for both formulations. However, increasing CM11:PLGA to 0.05 increases EE% only slightly, indicating that particles are saturated at this weight ratio. The maximum EE% for NPCM11 and MPCM11 at CM11:PLGA=0.05 were 63.5% and 60.3%, respectively. For both formulations, LC% declined continuously with increasing CM11:PLGA, reaching as low as 0.3% at CM11:PLGA = 0.05.

Table 3. Values of encapsulation efficiency (EE%) and loading capacity (LC%) for different peptide to polymer (CM11: PLGA) weight ratios

Sample	CM11:PLGA (w/w)	Encapsulation efficiency % (EE%)	Loading capacity % (LC%)
NPCM11	0.005	26.9 ±11.0	1.3±0.2
	0.01	57.8±6.3	0.6±0.5
	0.05	63.5±4.9	0.3±0.1
MPCM11	0.005	24.9±7.8	1.2±0.3
	0.01	56.7±5.5	0.6±0.4
	0.05	60.3±8.3	0.3±0.2

In vitro CM11 release assay

Figure 6 demonstrates the release profile of CM11 from NPCM11 and MPCM11 over the course of 192 hr *in vitro*. Generally, NPCM11 demonstrated a higher release rate than MPCM11, with a larger portion of CM11 released over the test period. In the first 12 hr, the amount of burst release for NPCM11 and MPCM11 was 39% and 30%, respectively. For NPCM11, 48% of CM11 was released in the first 24 hr, which was 12% higher than that of MPCM11. In the next 168 hr, NPCM11 consistently released more of its payload and reached over 80% cumulative release. The release rate for MPCM11, on the other hand, was slower, and cumulative release reached roughly 60% by the end of the test.

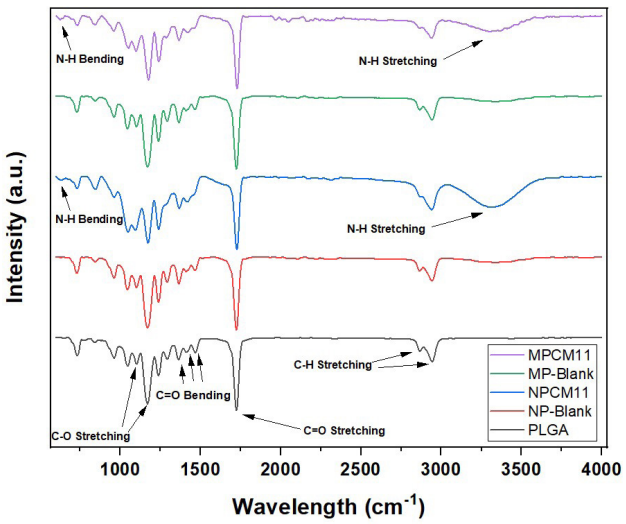

Figure 5. Fourier transform infrared spectra of blank poly(lactic-co-glycolic acid) nanoparticles (NP-Blank) and microparticles (MP-Blank) and CM11-loaded poly(lactic-co-glycolic acid) nanoparticles (NPCM11) and microparticles (MPCM11)

Corrected Proof

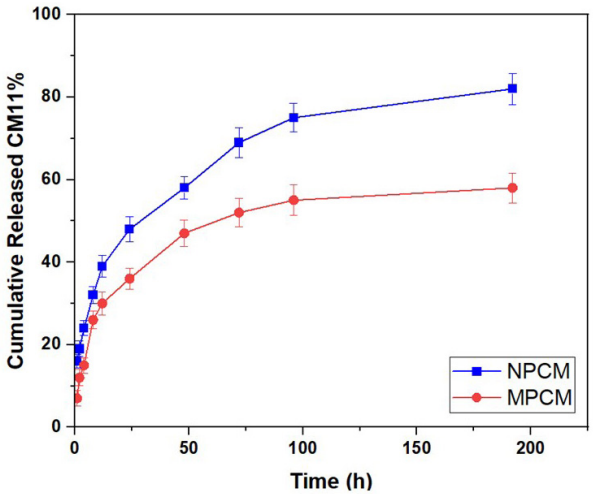

Figure 6. Release profile of CM11 from CM11-loaded poly(lactic-co-glycolic acid) nanoparticles (NPCM11) and microparticles (MPCM11)

MIC-MBC and biofilm inhibition assay

Table 4 reports the values of MIC/MBC obtained from the broth microdilution assay. The values for free CM11, NPCM11, and MPCM11 are reported as the concentration of CM11, whereas the values for NP-blank and MP-blank are reported as the concentration of PLGA. Neither NP-blank nor MP-blank exhibited antibacterial activity against any of the tested strains at the highest tested concentration (>14 mg/ml PLGA). For *E. coli*, NPCM11 demonstrated the lowest MIC (8 µg/ml), whereas free CM11 and MPCM11 exhibited MIC values of 32 µg/ml. For *S. aureus*, the MIC values of free CM11 and NPCM11 were identical (32 µg/ml), while MPCM11 exhibited a higher MIC of 64 µg/ml. Against *P. aeruginosa*, free CM11 and NPCM11 showed identical MIC values (16 µg/ml), whereas MPCM11 exhibited an MIC of 32 µg/ml. A similar pattern was observed for the MBC values.

Table 4. Minimum inhibitory concentration (MIC)/minimum bactericidal concentration (MBC) values from broth microdilution assay

Bacterial strain	Formulation	MIC	MBC
	Free CM11	32 µg/ml	64 µg/ml
	CM11-loaded nanoparticle	8 µg/ml	32 µg/ml
E. coli	CM11-loaded microparticle	32 µg/ml	64 µg/ml
	Blank nanoparticle	>14 mg/ml	>14 mg/ml
	Blank microparticle	>14 mg/ml	>14 mg/ml
	Free CM11	32 µg/ml	64 µg/ml
	CM11-loaded nanoparticle	32 µg/ml	32 µg/ml
S. aureus	CM11-loaded microparticle	64 µg/ml	128 µg/ml
	Blank nanoparticle	>14 mg/ml	>14 mg/ml
	Blank microparticle	>14 mg/ml	>14 mg/ml
	Free CM11	16 µg/ml	32 µg/ml
	CM11-loaded nanoparticle	16 µg/ml	64 µg/ml
P. aeruginosa	CM11-loaded microparticle	32 µg/ml	128 µg/ml
	Blank nanoparticle	>14 mg/ml	>14 mg/ml
	Blank microparticle	>14 mg/ml	>14 mg/ml

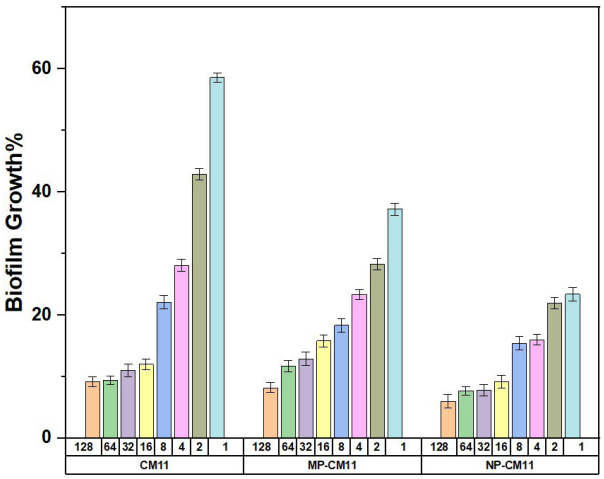

Figure 7. Results of *Pseudomonas aeruginosa* biofilm inhibition assay reported as growth percentage of biofilm for each formulation at different concentrations (µg/ml)

Figure 7 reports the results of the *P. aeruginosa* biofilm inhibition assay for each formulation and concentration based on growth percentage relative to the positive control group. At higher concentrations, NPCM11 produced the greatest reduction in biofilm biomass, followed by MPCM11 and free CM11. This trend was also observed at intermediate concentrations, where both particulate formulations generally resulted in lower biofilm growth percentages than free CM11. At the lowest tested concentrations, the inhibitory effects of all formulations were reduced.

MTT assay

The results of the MTT assay for investigating biocompatibility of formulations can be observed in Figure 8. Statistical analysis by calculating *P*-values was employed to assess the level of cytotoxicity of each formulation. As shown in Figure 8, free CM11 induced significant cytotoxicity at all tested concentrations compared with the control group. Encapsulation of CM11 in MPs markedly reduced its cytotoxicity, with no significant toxicity observed even at 500 µg/ml. NP encapsulation also reduced CM11-induced cytotoxicity up to 250 µg/ml; however, NPCM11 remained cytotoxic at 500 µg/ml. NP-blank and MP-blank showed no significant cytotoxicity compared with the control group.

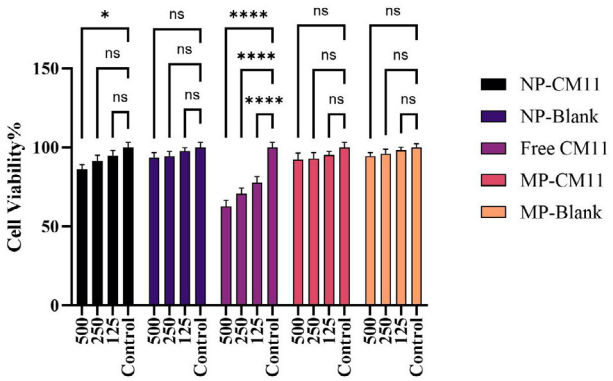

Figure 8. MTT Assay with Human Foreskin Fibroblasts (HFF) cell line for free CM11, blank nanoparticles (NP-Blank) and microparticles (MP-Blank), and CM11-loaded nanoparticles (NPCM11) and microparticles (MPCM11)
ns: non-significant, **P-value*<0.05, *****P-value*<0.0001) – X-axis denotes different concentrations (µg/ml)

Corrected Proof

Discussion

Based on the results of single-factor analysis from Table 1, the power and duration of the ultrasonic probe and O:W2 ratio are the main parameters that determine whether the protocol yields NPCM11 or MPCM11. Compared with S1, cutting duration and power input of the ultrasonic probe by 50% in S4 and S6, respectively, led to an increase in Z-average from 281 nm (S1) to 334 nm (S4) and 349 nm (S6). In S8, all parameters, including O:W2, PVA %w/v, ultrasonic power, ultrasonic time, and PLGA concentration, were shifted to favor MP formation. However, even the lowest power input (80 W) for 30 sec of ultrasonic probe exposure led to the formation of NPs (Z-average=323 nm). Therefore, to synthesize MPCM11, the ultrasonic technique was replaced with vigorous vortexing to minimize size reduction, while ensuring uniform emulsion droplet formation and distribution. Regarding O:W2, comparing S9 and S10 indicates a negative correlation between this parameter and PDI, meaning that higher O:W2 ratios are favored for monodispersity. Additionally, the significant increase in Z-average in S3 compared with S1 can be attributed to the decline of O:W2 from 0.5 to 0.2. Overall, these results advocate for higher O:W2 ratios for both MPCM11 and NPCM11.

Regarding the stability studies, the small changes in the zeta potential of S1 over four weeks likely reflect normal physicochemical fluctuations during storage, such as minor surface rearrangement of the PLGA matrix, rather than substantial alterations in particle surface properties. DLS measurements were not performed for S11 during the stability study because the technique is not well suited for accurate sizing of micron-scale particles (29). Therefore, the stability of S11 was assessed by FESEM through comparison of particle morphology and size before and after storage.

Regarding CM11 encapsulation, to make a compromise between EE% and LC%, CM11:PLGA=0.01 is a more appropriate choice, maintaining higher values of both parameters compared with higher or lower levels of CM11:PLGA. Overall, the LC% values are very low. This was expected since we decided to use a high concentration of PLGA to achieve higher EE%. This approach has been reported in the literature (36).

We compared the release profile of NPCM11 and MPCM11 with several other particulate-based formulations reported in the literature. Moosazadeh Moghaddam *et al.* (10) studied chitosan NPs for CM11 delivery to treat *Helicobacter pylori*. In that study, roughly 60% of CM11 was released in 96 hr *in vitro*. Our PLGA formulation extended the duration of release twofold and increased the fraction of released CM11 by approximately 33%. Ali *et al.* (37) studied the *in vitro* release of SAAP-148 from PLGA NPs and observed a burst release of 50% within just 5 hr, which is considerably uncontrolled compared with our 39% burst release within 12 hr. The significantly lower size of their NPs (<100 nm) could be responsible for such a pronounced burst release. Water *et al.* (38) studied the *in vitro* release of plectasin from PLGA NPs at different LC% values (0.625, 1.25, 2.5%) and observed a negative correlation between LC% and burst release. Nonetheless, all nanoformulations demonstrated burst release levels above 70% in the first hour. Sharma *et al.* (39) studied the *in vitro* release of HHC10 peptide from PLGA NPs and observed roughly 45% burst release in less than 12 hr and nearly complete release of the peptide in a week. Cheng *et al.* (13) studied the *in vitro* release of OP-145 peptide from PLGA MPs and observed a 40% burst release in the first hours, with 80% of the peptide released in just three days. Compared with many reports of AMPs in the literature, our formulation has alleviated the burst release while prolonging the overall duration of release.

The range of MIC and MBC values obtained from the broth microdilution assay was in agreement with the ranges reported by Moosazadeh Moghaddam *et al.* (11). They conducted experiments on 30 to 40 clinical isolates of each investigated strain from Table 4. The obtained MIC values ranged from 2 to 64 µg/mL, depending on the isolate. NPCM11 consistently matched or outperformed free CM11. This finding indicates that NPCM11 not only preserves CM11 activity but can also enhance its effective interaction with bacterial cells under planktonic conditions. NPCM11 provides a favorable balance between protection and bioavailability. A fraction of CM11 is shielded from early degradation or nonspecific binding, while sufficient peptide is released rapidly enough to exert antimicrobial effects within the assay timeframe (24 hr). In addition, the colloidal stability of NPCM11 allows it to remain suspended and in proximity to planktonic bacteria, potentially increasing the local concentration of released CM11 at the bacterial membrane. Together, these effects explain why NPCM11 can display equal or superior apparent activity compared with free CM11 despite the latter being fully available throughout the incubation period. Although full availability is beneficial for rapid growth inhibition, it makes free CM11 susceptible to degradation and loss of antimicrobial activity during the incubation period. Dos Santos *et al.* (36) investigated antifungal activity of a synthetic peptide, Ctn (15-34), in free form and nanoformulation and observed a similar trend of superiority of the nanoformulation to the free drug. Compared with the free drug, the nanoformulation decreased yeast cell viability by 75%. Sharma *et al.* (39) encapsulated HHC10 peptide in PLGA NPs and studied its antimicrobial activity against *E. coli*. *In vitro* antibacterial testing revealed that while free HHC10 and the nanoformulation show similar antibacterial effects at low concentrations, the superiority of the nanoformulation becomes noticeable at higher concentrations of HHC10.

In contrast, MPCM11 exhibited reduced apparent activity in terms of MIC/MBC values relative to both free CM11 and NPCM11. This outcome reflects the intended function of MPs as long-acting depot systems rather than immediate inhibitors of planktonic growth. MPCM11 releases CM11 more slowly and tends to sediment under static assay conditions, limiting early peptide–bacterium contact and delaying the attainment of inhibitory concentrations. As a result, MPCM11 is intrinsically disadvantaged in short-term planktonic assays like broth microdilution that emphasize rapid growth inhibition and peak drug exposure (40). Jiao *et al.* (41) evaluated antimicrobial activity of OH-CATH30 peptide in free form and microformulation against *E. coli*, *S. aureus*, and *P. aeruginosa*. In all cases, the microformulation demonstrated comparable or slightly inferior antimicrobial activity to the free peptide.

An exception to the overall trend was observed for *E. coli*, where NPCM11 exhibited a markedly lower MIC than free CM11. This strain-specific enhancement reflects features of the Gram-negative outer membrane that favor NP-mediated

Corrected Proof

peptide delivery. In *E. coli*, adsorption of NPCM11 to the lipopolysaccharide (LPS)-rich surface may increase the local concentration of released peptide at the bacterial envelope, partially overcoming permeability barriers and reducing susceptibility to peptide degradation (42, 43). Such effects would be less pronounced in *S. aureus*, which lacks an outer membrane, and in *P. aeruginosa*, which possesses additional AMP resistance mechanisms.

Importantly, the absence of antibacterial activity in NP-blank and MP-blank confirms that these trends arise from differences in CM11 availability rather than any contribution from the polymeric carrier. The divergent performances of NPCM11 and MPCM11 underscore a central principle of antimicrobial drug delivery: particle size governs the balance between immediate efficacy and sustained exposure (44). The results indicate that NPCM11 occupies an intermediate regime in which the CM11 release pattern is compatible with the temporal demands of MIC/MBC assays, whereas MPCM11 prioritizes prolonged release at the expense of early effectiveness.

The key difference between this assay and the broth microdilution assay was the use of flat-bottom 96-well plates instead of U-bottom ones. We made this difference because flat surfaces are better at promoting cell adhesion and consequent biofilm formation. Regarding the biofilm inhibition assay, the antibacterial efficiency of free CM11 observed from MIC/MBC values can be attributed to its immediate bioavailability and rapid membrane disruption against planktonic bacteria. However, while highly effective in inhibiting planktonic growth due to its immediate bioavailability, free CM11 is susceptible to degradation, adsorption, and neutralization during incubation, leading to a decline in its effective concentration over time. This loss of sustained antimicrobial effectiveness allows surviving bacteria to attach to the surface and initiate biofilm formation. Additionally, free CM11 is susceptible to rapid inactivation by extracellular polymeric substances (EPS) and proteolytic enzymes secreted by the biofilm. In contrast, NPCM11 and MPCM11 provide a continuous release of the peptide throughout the incubation period, maintaining inhibitory concentrations during critical stages of surface attachment and biofilm development (40, 45). Consequently, both of the particulate formulations demonstrate superior biofilm inhibition to free CM11. Cresti *et al.* (46) studied the antibiofilm activity of SET-M33, encapsulated in PLGA NPs, against *P. aeruginosa*. The nanoformulation demonstrated antibiofilm activity comparable to free SET-M33.

The biofilm inhibition profiles further highlight the functional distinction between NPCM11 and MPCM11. While both formulations suppress biofilm formation more effectively than free CM11 across the tested concentration range, NPCM11 consistently exhibits stronger inhibition than MPCM11, particularly at lower and intermediate concentrations. This behavior reflects differences in how the two systems deliver CM11 during the dynamic, multistage process of biofilm development. NPCM11 remains well dispersed in the culture medium. It is more likely to interact with bacterial cells during early attachment and biofilm formation, enabling a more uniform and sustained distribution of released CM11 at the cell–surface interface. In contrast, MPCM11 tends to sediment and act as a localized depot, releasing CM11 more slowly and less uniformly throughout the well (41). Although this sustained release is sufficient to inhibit biofilm formation relative to free CM11, it provides weaker and spatially heterogeneous antimicrobial pressure compared with NPCM11, particularly during the early stages when attachment and EPS production are initiated. Consequently, NPCM11 more effectively disrupts the processes that contribute to biofilm biomass accumulation, whereas MPCM11 exerts a delayed but still beneficial inhibitory effect. These results reinforce the conclusion that NPCM11 is better suited for interfering with biofilm initiation under planktonic-to-surface transition conditions. At the same time, MPCM11 functions as a longer-term reservoir whose advantages become more pronounced in applications requiring prolonged local delivery rather than maximal early inhibition.

Because the formulations were added simultaneously with the bacterial inoculum, the biofilm inhibition assay cannot fully distinguish between inhibition of biofilm formation and inhibition of planktonic bacterial growth. Therefore, the reduced biofilm biomass observed at concentrations equal to or greater than the MIC may be partially attributable to growth inhibition. Nevertheless, the assay remains useful for evaluating the overall ability of the formulations to prevent biofilm establishment during the early stages of bacterial attachment and development, especially in concentrations below the MIC. Hence, according to MIC values from Table 4, the biofilm inhibition effects observed at concentrations below 16 µg/mL for free CM11 and NPCM11, and below 32 µg/mL for MPCM11 can be attributed to the biofilm inhibition capacity of the formulations.

It should be noted that a 24 hr incubation period is generally insufficient to establish a mature biofilm and, therefore, does not support conclusions about the eradication of preformed biofilms. Our intention was not to evaluate biofilm eradication. Instead, we aimed to determine whether free CM11, NPCM11, and MPCM11 could inhibit biofilm formation during the initial stages of bacterial attachment and biofilm development. Accordingly, the assay was intentionally designed as a biofilm inhibition assay, in which the formulations were added simultaneously with the bacterial inoculum and remained present throughout the 24 hr incubation period.

Regarding the MTT assay, the more pronounced cytotoxic effects of NPCM11 compared with MPCM11 at 500 µg/mL can be attributed to a higher release rate of CM11 from NPCM11. The faster release results in HFF cells being exposed to a higher concentration of CM11 during the assay.

Conclusion

NPCM11 and MPCM11 were successfully developed and characterized as potential delivery systems for treating *P. aeruginosa* infections. Both formulations exhibited sustained peptide release and enhanced inhibition of biofilm formation compared with free CM11. In antimicrobial susceptibility testing, NPCM11 demonstrated superior antibacterial activity to MPCM11. Among the tested formulations, NPCM11 showed the most favorable overall performance against both planktonic bacteria and biofilm formation. These findings suggest that NP-based delivery of CM11 may be a promising strategy to improve the therapeutic efficacy of AMPs against *P. aeruginosa* infections. Further studies are warranted to evaluate the *in vivo* performance and therapeutic potential of these formulations.

Corrected Proof

Acknowledgment

We thank the Clinical Research Development Unit of Baqiyatallah Hospital for its guidance and advice. We want to thank the Research and Technology Comprehensive Laboratory (RTCL) of Baqiyatallah University of Medical Sciences, Iran, for its guidance and support.

Funding

The funding for this research was provided by Baqiyatallah University of Medical Sciences, Iran.

Authors' Contributions

M E, MM M, M D, NJ J, H H, and RA T contributed to study conception and design. M E performed experiments and collected data. M E, M D, and RA T interpreted and analyzed the results. M E prepared the manuscript and visualized the results. MM M, M D, NJ J, H H, and RA T revised and edited the article. MM M, NJ J, and H H supervised the project and decisions regarding its direction. RA T was responsible for funding acquisition.

Conflicts of Interest

The authors declare no conflicts of interest.

Declaration

We have not used any AI tools or technologies to prepare this manuscript.

References

1. Naghavi M, Vollset SE, Ikuta KS, Swetschinski LR, Gray AP, Wool EE, *et al*. Global burden of bacterial antimicrobial resistance 1990–2021: A systematic analysis with forecasts to 2050. Lancet 2024; 404: 1199-226.
2. Kerr KG, Snelling AM. *Pseudomonas aeruginosa*: A formidable and ever-present adversary. J Hosp Infect 2009; 73: 338-344.
3. Mulcahy LR, Isabella VM, Lewis K. *Pseudomonas aeruginosa* biofilms in disease. Microb Ecol 2014; 68: 1-2.
4. Pang Z, Raudonis R, Glick BR, Lin TJ, Cheng Z. Antibiotic resistance in *Pseudomonas aeruginosa*: Mechanisms and alternative therapeutic strategies. Biotechnol Adv 2019; 37: 177-192.
5. Huan Y, Kong Q, Mou H, Yi hr. Antimicrobial peptides: Classification, design, application and research progress in multiple fields. Front Microbiol 2020; 11: 582779.
6. Zhang QY, Yan ZB, Meng YM, Hong XY, Shao G, Ma JJ, *et al*. Antimicrobial peptides: Mechanism of action, activity and clinical potential. Mil Med Res 2021; 8: 48.
7. Xuan J, Feng W, Wang J, Wang R, Zhang B, Bo L, *et al*. Antimicrobial peptides for combating drug-resistant bacterial infections. Drug Resist Update 2023; 68: 100954.
8. Ali M, Garg A, Srivastava A, Arora PK. The role of antimicrobial peptides in overcoming antibiotic resistance. Microbe 2025; 7: 100337.
9. Amani J, A. Barjini K, M. Moghaddam M, Asadi A. *In vitro* synergistic effect of the CM11 antimicrobial peptide in combination with common antibiotics against clinical isolates of six species of multidrug-resistant pathogenic bacteria. Protein Peptide Lett 2015; 22: 940-951.
10. Moosazadeh Moghaddam M, Bolouri S, Golmohammadi R, Fasihi-Ramandi M, Heiat M, Mirnejad R. Targeted delivery of a short antimicrobial peptide (CM11) against *Helicobacter pylori* gastric infection using concanavalin A-coated chitosan nanoparticles. J Mater Sci Mater Med 2023; 34: 44.
11. Moosazadeh Moghaddam M, Abolhassani F, Babavalian H, Mirnejad R, Azizi Barjini K, Amani J. Comparison of *in vitro* antibacterial activities of two cationic peptides CM15 and CM11 against five pathogenic bacteria: *Pseudomonas aeruginosa*, *Staphylococcus aureus*, *Vibrio cholerae*, *Acinetobacter baumannii*, and *Escherichia coli*. Probiotics Antimicrob Proteins 2012; 4: 133-139.
12. Heiat M, Aghamollaei H, Moghaddam MM, Kooshki hr. Using CM11 peptide as a cell permeable agent for the improvement of conventional plasmid transformation methods in *Escherichia coli* and *Bacillus subtilis*. Minerva Biotecnol 2014; 26: 149-157.
13. Cheng Y, Qin J, Huang Y, Wang T. The antimicrobial effects of PLGA microspheres containing the antimicrobial peptide OP-145 on clinically isolated pathogens in bone infections. Sci Rep 2022; 12: 14541.
14. Jiao X, Dong X, Shan H, Qin Z. Assessing the efficacy of PLGA-loaded antimicrobial peptide OH-CATH30 microspheres for the treatment of bacterial keratitis: a promising approach. Biomolecules 2023; 13: 1244.
15. Carnero Canales CS, Roque-Borda CA, Cazorla JI, Cazorla RM, Apaza UJ, Silva VD, *et al*. Forging a new frontier: Antimicrobial peptides and nanotechnology converging to conquer gastrointestinal pathogens. Small 2025; 21: 2501431.
16. Khademi F, Sahebkar A, Fasihi-Ramandi M, Taheri RA. Induction of strong immune response against a multicomponent antigen of *Mycobacterium tuberculosis* in BALB/c mice using PLGA and DOTAP adjuvant. AAMS 2018; 126: 509-514.
17. Eshaghi M, Dehghani M, Abedi A, Moosazadeh Moghaddam M, Taheri RA. Poly (lactic-co-glycolic acid) nanoparticles and microparticles for peptide delivery: Release mechanisms and controlling factors. ADMET DMPK 2026; 14: 3091.
18. Nkansah MK, Cheng SY, Holdt AM, Lavik EB. Poly (lactic-co-glycolic acid) nanospheres and microspheres for short- and long-term delivery of bioactive ciliary neurotrophic factor. Biotechnol Bioeng 2008; 100: 1010-1019.
19. Panyam J, Dali MM, Sahoo SK, Ma W, Chakravarthi SS, Amidon GL, *et al*. Polymer degradation and *in vitro* release of a model protein from poly (D, L-lactide-co-glycolide) nano-and microparticles. J Control Release 2003; 92: 173-187.
20. Chen W, Hu S. Suitable carriers for encapsulation and distribution of endostar: Comparison of endostar-loaded particulate carriers. Int J Nanomed 2011; 22: 1535-1541.
21. Wu H, Moser C, Wang HZ, Høiby N, Song ZJ. Strategies for combating bacterial biofilm infections. Int J Oral Sci 2015; 7: 1-7.
22. Shi D, Mi G, Wang M, Webster TJ. *In vitro* and *ex vivo* systems at the forefront of infection modeling and drug discovery. Biomaterials 2019; 198: 228-249.
23. Furukawa S, Kuchma SL, O'toole GA. Keeping their options open: Acute versus persistent infections. J Bacteriol 2006; 188: 1211-1217.
24. McCall RL, Sirianni RW. PLGA nanoparticles formed by single-or double-emulsion with vitamin E-TPGS. J Vis Exp 2013; 82: 51015.
25. Oyaghire SN, Quijano E, Piotrowski-Daspit AS, Saltzman WM, Glazer PM. Poly (lactic-co-glycolic acid) nanoparticle delivery of peptide nucleic acids *in vivo*. Methods Mol Biol 2020; 2105: 261-281.
26. Haque S, Boyd BJ, McIntosh MP, Pouton CW, Kaminskas LM, Whittaker M. Suggested procedures for the reproducible synthesis of poly (d, l-lactide-co-glycolide) nanoparticles using the emulsification solvent diffusion platform. Curr Nanosci 2018; 14: 448-453.
27. Kızılbey K. Optimization of rutin-loaded PLGA nanoparticles synthesized by single-emulsion solvent evaporation method. ACS Omega 2019; 4: 555-562.
28. Jia-Gen W, Tingting G, Hong-Yuan Z, Yi-Yun X, Xiu-Zhen Z, Guo C, *et al*. Preparation and optimization of PEG-PLGA loaded with vincristine sulfate and its *in vitro* release. J Bioequiv Avail 2011; 3: 211-214.
29. Filippov SK, Khusnutdinov R, Murmiliuk A, Inam W, Zakharova LY, Zhang H, *et al*. Dynamic light scattering and transmission electron microscopy in drug delivery: A roadmap for correct characterization of nanoparticles and interpretation of results. Mater Horiz 2023; 10: 5354-5370.
30. CLSI C. Performance standards for antimicrobial susceptibility

Corrected Proof

testing. Clinical Lab Standards Institute 2016; 35: 16-38.
31. Haney EF, Trimble MJ, Hancock RE. Microtiter plate assays to assess antibiofilm activity against bacteria. Nat Protoc 2021; 16: 2615-2632.
32. Singh R, Kesharwani P, Mehra NK, Singh S, Banerjee S, Jain NK. Development and characterization of folate anchored Saquinavir entrapped PLGA nanoparticles for anti-tumor activity. Drug Dev Ind Pharm 2015; 41: 1888-1901.
33. Singh G, Kaur T, Kaur R, Kaur A. Recent biomedical applications and patents on biodegradable polymer-PLGA. Int J Pharmacol Pharm Sci 2014; 1: 30-42.
34. Saucedo-Balderas MM, Delgado-Alfaro RA, MartínezMartínez FJ, Ortegón-Reyna D, Bernabé-Pineda M, Zúñiga-Lemus O, *et al.* Synthesis, molecular structure of diethyl phenylenebis (Methylene) dicarbamates and FTIR spectroscopy molecular recognition study with benzenediols. J Brazil Chem Soc 2015; 26: 396-402.
35. Aboul-eneın Y, Bunacıu A, Fleschın S. Evaluation of the protein secondary structures using Fourier transform infrared spectroscopy. Gazi Univ J Sci 2014; 27: 637-644.
36. Dos Santos AP, Oliveira RC, Louchard BO, Uchoa AF, Ricardo NM, Leal LK, *et al.* Preparation of PLGA nanoparticles loaded with the anti-infective Ctn (15-34) peptide for antifungal application. Braz Arch Biol Tech 2023; 66: e20220775.
37. Ali M, van Gent ME, de Waal AM, van Doodewaerd BR, Bos E, Koning RI, *et al.* Physical and functional characterization of PLGA nanoparticles containing the antimicrobial peptide SAAP-148. Int J Mol Sci 2023; 24: 2867.
38. Water JJ, Smart S, Franzyk H, Foged C, Nielsen HM. Nanoparticle-mediated delivery of the antimicrobial peptide plectasin against *Staphylococcus aureus* in infected epithelial cells. Eur J Pharm Biopharm 2015; 92: 65-73.
39. Sharma A, Vaghasiya K, Ray E, Verma RK. Nano-encapsulated HHC10 host defense peptide (HDP) reduces the growth of Escherichia coli via multimodal mechanisms. Artif Cells Nanomed Biotechnol 2018; 46: 156-165.
40. Wang L, Hu C, Shao L. The antimicrobial activity of nanoparticles: Present situation and prospects for the future. Int J Nanomed 2017; 12: 1227-49.
41. Jiao X, Dong X, Shan H, Qin Z. Assessing the efficacy of PLGA-loaded antimicrobial peptide OH-CATH30 microspheres for the treatment of bacterial keratitis: A promising approach. Biomolecules 2023; 13: 1244.
42. Shakya AK, Al-Sulaibi M, Naik RR, Nsairat H, Suboh S, Abulaila A. Review on PLGA polymer based nanoparticles with antimicrobial properties and their application in various medical conditions or infections. Polymers 2023; 15: 3597.
43. Birk SE, Boisen A, Nielsen LH. Polymeric nano-and microparticulate drug delivery systems for treatment of biofilms. Adv Drug Deliver Rev 2021; 174: 30-52.
44. Sandri G, Bonferoni MC, Ferrari F, Rossi S, Caramella CM. The role of particle size in drug release and absorption. InParticulate Products: Tailoring Properties for Optimal Performance 2013; 323-341. Cham: Springer International Publishing.
45. Shariati A, Chegini Z, Ghaznavi-Rad E, Zare EN, Hosseini SM. PLGA-based nanoplatforms in drug delivery for inhibition and destruction of microbial biofilm. Front Cell Infect Microbiol 2022; 12: 926363.
46. Cresti L, Conte C, Cappello G, Brunetti J, Falciani C, Bracci L, *et al.* Inhalable polymeric nanoparticles for pulmonary delivery of antimicrobial peptide SET-M33: Antibacterial activity and toxicity *in vitro* and *in vivo*. Pharmaceutics 2023; 15: 3.

Corrected Proof